

Bound states of a ferromagnetic wire in a superconductor

Jay D. Sau* and P. M. R. Brydon†

Condensed Matter Theory Center and Joint Quantum Institute,
University of Maryland, College Park, Maryland 20742-4111, USA

(Dated: January 16, 2015)

We consider the problem of bound states in strongly anisotropic ferromagnetic impurities in a superconductor, motivated by recent experiments that claim to observe Majorana modes at the ends of ferromagnetic wires on a superconducting substrate [S. Nadj-Perge *et al.*, Science **346**, 602 (2014)]. Generalizing the successful theory of bound states of spherically symmetric impurities, we consider a wire-like potential using both analytical and numerical approaches. We find that away from the ends of the wire the bound states form bands with pronounced van Hove singularities, giving rise to subgap peaks in the local density of states. For sufficiently strong magnetization of the wire, we show that this process generically produces a sharp peak at zero energy in the local density of states near the ends of the wire. This zero-energy peak has qualitative similarities to the claimed signature of a Majorana mode observed in the aforementioned experiment.

PACS numbers: 74.25.Ha, 73.20.Hb

Introduction. The antagonistic relationship between superconductivity and ferromagnetism manifests itself in many diverse ways. For example, it has long been known that a magnetic impurity in a superconductor supports bound states with energy within the superconducting gap [1–3]. These Yu-Shiba-Rusinov (YSR) states can be directly imaged using scanning tunneling microscopy (STM) techniques [4, 5]. They have been extensively studied [6], and play a key role in a wide range of phenomena such as Kondo-Andreev screening [7] and mediating long-ranged antiferromagnetic exchange interactions [8]. Very recently, the bands formed by overlapping YSR states in an array of magnetic impurities has attracted great attention as a way to engineer a topological superconductor with Majorana edge modes [9–16]. Realizing a Majorana mode is not only of fundamental interest, but also of technological importance, as their non-Abelian braiding statistics is key to promising proposals to build a quantum computer [17].

Much excitement has therefore been generated by recent claims of the observation of Majorana modes in a ferromagnetic wire on a superconducting substrate [18]. Specifically, STM measurements reveal a sharply-localized peak at zero-bias in the local density of states (LDOS) at the ends of atomically-thin iron wires grown on a lead surface, which are interpreted as Majorana bound states. Several theoretical calculations [19–21] have shown that as a matter of principle Majorana modes can occur in such a ferromagnetic wire on a superconductor in the presence of spin-orbit coupling (SOC), in much the same way as had been suggested in more mesoscopic geometries [22–26].

A characteristic aspect of the experimental results is that the LDOS in the wire shows pronounced subgap features, which resemble the spectrum of YSR states

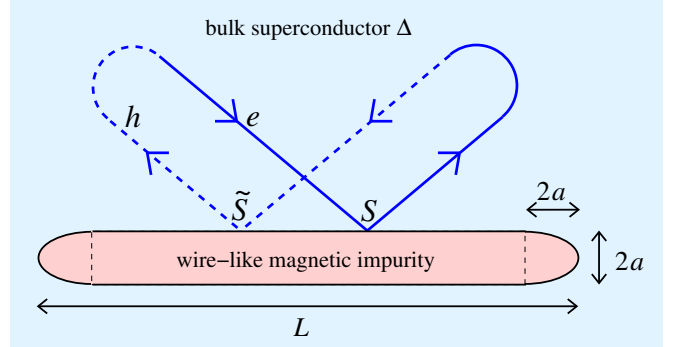


Figure 1. (Color online) We consider a wire-like magnetic impurity embedded in a bulk superconductor with gap Δ . The wire has length L and radius a , with half-ellipsoidal caps at each end with major (minor) axis $4a$ ($2a$). We schematically show a YSR state as the scattering of an electron quasiparticle (solid line) at the impurity followed by its Andreev reflection as a hole, and its subsequent scattering and Andreev scattering. Electrons and holes undergo conventional reflection at the magnetic impurity, described by the scattering matrices S and \tilde{S} , respectively. The difference in phase for electron- and hole-scattering off the magnetic impurity is compensated by the energy-dependent phase acquired by perfect Andreev reflection in the superconductor.

previously observed in isolated magnetic impurities or dimers [4, 5]. This motivates us to go beyond the usual models of a spherical magnetic impurity [1–3, 6], and consider the ferromagnetic wire itself as a highly anisotropic scattering center. Our approach overcomes the limitations of studying wire-like magnetic impurities using simple quasi-two-dimensional tight-binding models [18, 21], and hence allows us to develop a more general understanding of the behavior of YSR states in these systems. In particular, we wish to investigate whether or not the subgap features interpreted as Majorana modes in Ref. 18 could have a conventional nontopological origin.

In this letter we present a study of the YSR states

* jaydsau@umd.edu

† pbrydon@umd.edu

in a ferromagnetic wire-like impurity with smooth ends, shown schematically in Fig. (1). We start by developing a general approach for obtaining the energies and wavefunctions of the YSR states in terms of an eigenvalue problem involving the normal-state scattering matrices. We apply this formalism to a long wire-like ferromagnetic impurity and calculate the energy spectra analytically using a semiclassical approximation. This reveals that the YSR bands in the wire typically possess van Hove singularities which would appear as strong peaks in the LDOS of the wire. As the wire tapers to its end, these features move towards the gap edges. For sufficiently strong magnetization of the wire, the van Hove singularities of the two particle-hole conjugated branches must cross at zero energy, giving a sharply-localized peak in the LDOS near the wire end. We confirm these theoretical expectations by direct numerical computation of the scattering matrix of the impurity using the T -matrix approach. In particular, the numerical results for the LDOS qualitatively resemble key features of the experiment [18]. Finally, applying our formalism to the case of impurities with SOC, we find that ferromagnetic wire may be expected to support Majorana modes with a small energy gap.

Scattering matrix formalism for bound states. Let us first examine the construction of a bound state wavefunction localized at a magnetic impurity in a superconductor, so that the energy lies within the gap, i.e. $|E| < \Delta$. Parametrizing the bound state energy through $E = \Delta \cos \varphi$, away from the impurity the wave function of the bound state satisfies the equation

$$-\left(\frac{\hbar^2 \nabla^2}{2m} + \mu\right) \psi = \Delta(-i\tau_y + \cos \varphi \tau_z) \psi, \quad (1)$$

where m is the effective mass and μ the chemical potential in the bulk superconductor. The solution can be expanded in eigenstates $(1, e^{\pm i\varphi})^T$ of the matrix $(-i\tau_y + \cos \varphi \tau_z)$ and angular momentum channels

$$\begin{aligned} \psi(\mathbf{r}) = & \sum_{l,m,\sigma} \left\{ h_l^{(-)}(k_- r) a_{l,m,\sigma} \begin{pmatrix} 1 \\ e^{i\varphi} \end{pmatrix} \right. \\ & \left. + h_l^{(+)}(k_+ r) b_{l,m,\sigma} \begin{pmatrix} 1 \\ e^{-i\varphi} \end{pmatrix} \right\} Y_l^m(\hat{\mathbf{r}}) \zeta_\sigma, \quad (2) \end{aligned}$$

where $a_{l,m,\sigma}$ and $b_{l,m,\sigma}$ are the scattering coefficients, ζ_σ is a spinor, and the Hankel functions satisfy

$$-\left(\frac{\hbar^2 \nabla^2}{2m} + \mu\right) h_l^{(\pm)}(k_\pm r) = \pm i\Delta \sin \varphi h_l^{(\pm)}(k_\pm r), \quad (3)$$

with $k_\pm = [2m(\mu \pm i\Delta \sin \varphi)]^{1/2}/\hbar$. In the asymptotic limit $|k_\pm| r \gg 1$, and with $\mu \gg \Delta$, we can approximate

$$\begin{aligned} \psi(\mathbf{r}) \approx & \frac{e^{-\frac{r\Delta \sin \varphi}{\hbar v_F}}}{k_F r} \sum_{l,m,\sigma} \left\{ e^{-i[k_F r - (l+1)\pi/2]} a_{l,m,\sigma} \begin{pmatrix} 1 \\ e^{i\varphi} \end{pmatrix} \right. \\ & \left. + e^{i[k_F r - (l+1)\pi/2]} b_{l,m,\sigma} \begin{pmatrix} 1 \\ e^{-i\varphi} \end{pmatrix} \right\} Y_l^m(\hat{\mathbf{r}}) \zeta_\sigma, \quad (4) \end{aligned}$$

where $v_F = \hbar k_F/m$ is the Fermi velocity and $k_F = \sqrt{2m\mu}/\hbar$ is the Fermi wavevector.

For $r \ll \xi = \hbar v_F/\Delta$ we may ignore the exponential decay in Eq. (4), and the form of $\psi(\mathbf{r})$ in the electron sector is then identical to the wave function for scattering off the impurity in the normal state. The coefficients therefore obey

$$b = S a, \quad (5)$$

where we have introduced a matrix-vector notation for the normal-state scattering matrix $S \equiv S_{l,m,\sigma;l',m',\sigma'}$, and the vectors $a \equiv a_{l,m,\sigma}$ and $b \equiv b_{l,m,\sigma}$. Similarly, the hole channel wave function is a normal scattering state for the time-reversed Hamiltonian $\tilde{H} = \sigma_y H^* \sigma_y$. Therefore, the vectors a, b also satisfy

$$e^{-2i\varphi} b = \tilde{S} a, \quad (6)$$

where the time-reversed scattering matrix \tilde{S} is given by $\tilde{S} = \Lambda \sigma_y S^T \sigma_y \Lambda^\dagger$ and Λ is the matrix that time-reverses the orbital indices. One obtains a and the phase φ , which determines the bound state energy $E = \Delta \cos \varphi$, by recasting Eqs. (5) and (6) as an eigenvalue problem

$$e^{-2i\varphi} a = S^\dagger \tilde{S} a. \quad (7)$$

The other scattering amplitude b is obtained from a using Eq. (5).

Equation (7) generalizes Rusinov's expression [3] for the YSR bound state for spherically symmetric impurities. In this case, the scattering matrix in each angular momentum channel (l, m) is written as $S_{l,m} = \text{diag}(e^{2i\delta_{l,\uparrow}}, e^{2i\delta_{l,\downarrow}})$. Solving Eq. (7), the bound state energy is then

$$E_{l,m,\sigma} = \sigma \Delta \cos(\delta_{l,\uparrow} - \delta_{l,\downarrow}). \quad (8)$$

where the sign σ is positive (negative) according as the state has spin aligned (antialigned) with the magnetic moment of the impurity.

Semiclassical theory for a ferromagnetic wire. We now turn our attention to a wire-like impurity, which we assume to lie along the z -axis. The scattering matrix can be estimated semiclassically, assuming that the wire is smooth on the scale of k_F^{-1} . This is satisfied for the experiment reported in [18], where in the lead substrate we have $k_F^{-1} \approx 0.13 a_{\text{Pb}}$, with a_{Pb} the lattice constant [27]. The small value of k_F^{-1} makes it reasonable to assume that the scattering potential changes sufficiently slowly along the wire such that the parallel component of quasi-particle momentum is approximately conserved. Regarding the wire-like Fe impurity as cylindrically symmetric, the calculation of the bound-state energies for fixed k_z reduces to the bound-state problem for an isotropic impurity in two dimensions. Setting the magnetic moment along the z -axis, the scattering matrix in each azimuthal angular momentum channel m is

$$S_m(k_z, z) = e^{i\phi_m(k_z, z)} e^{i b_m(k_z, z) \sigma_z}, \quad (9)$$

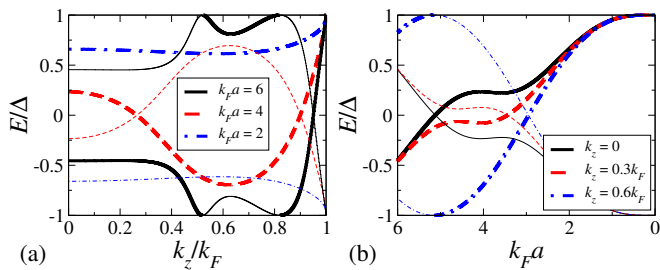


Figure 2. (Color online) Semiclassical results for the YSR energy bands in a magnetic wire. (a) Dispersion of the energy bands for different wire thicknesses a . (b) Dependence of the bound state energy on the wire thickness a at various fixed k_z . The spin- \uparrow (\downarrow) branch is represented by the thick (thin) lines. We set the potentials $V_\uparrow = 0.04\mu$ and $V_\downarrow = 0.6\mu$.

where the z -dependence arises from the varying potential of the impurity, which is assumed to be slow compared to k_F^{-1} . Reflection and spin-rotation invariance imply that $\phi_m(-k_z, -z) = \phi_m(k_z, z)$ and $b_m(-k_z, -z) = b_m(k_z, z)$. The time-reversed scattering matrix is

$$\tilde{S}_m(k_z, z) = e^{i\phi_m(k_z, z)} e^{-ib_m(k_z, z)\sigma_z}. \quad (10)$$

Solving for the eigenstates of $S^\dagger \tilde{S}$, the energy of the spin- σ state in the m channel is given by

$$E_{m,\sigma}(k_z, z) = \sigma \Delta \cos[b_m(k_z, z)]. \quad (11)$$

The phase shifts ϕ_m and b_m are the solutions of

$$\tan(\phi_m + \sigma b_m) = \frac{k_\sigma J_m(k_\perp a) \tilde{J}'_m(k_\sigma a) - k_\perp J'_m(k_\perp a) \tilde{J}_m(k_\sigma a)}{k_\sigma Y_m(k_\perp a) \tilde{J}'_m(k_\sigma a) - k_\perp Y'_m(k_\perp a) \tilde{J}_m(k_\sigma a)}, \quad (12)$$

where $k_\perp^2 = k_F^2 - k_z^2$, $k_\sigma^2 = |k_\perp^2 - k_F^2 V_\sigma/\mu|$ with V_σ the scattering potential experienced by spin- σ particles, $J_m(x)$ and $Y_m(x)$ are Bessel functions, and \tilde{J}_m is $J_m(x)$ or the modified Bessel function $I_m(x)$ according as the expression within the absolute value sign in the definition of k_σ^2 is positive or negative. The radius of the wire is denoted by a , and vanishes towards the ends.

We consider a magnetic potential sufficient to close the superconducting gap in the wire, i.e. the YSR bands cross zero energy. Typical results for the $m = 0$ bands in this case are shown in Fig. (2). We observe that the YSR bands generically have van Hove singularities, typically near $k_z = 0$, which will produce a strong peak in the LDOS [16]. Closer to $|k_z| = k_F$, on the other hand, the bands show greater velocity $\sim \Delta/k_F$ and thus give a weaker contribution to the LDOS. Moving towards the end of the wire, the reduction of the radius causes the bands to shift towards the gap edge, as shown in Fig. (2)(b). The van Hove singularity will therefore also shift around in the gap, and so the LDOS near the wire ends will be qualitatively different from that in the middle of the wire. We can get a handle on the length

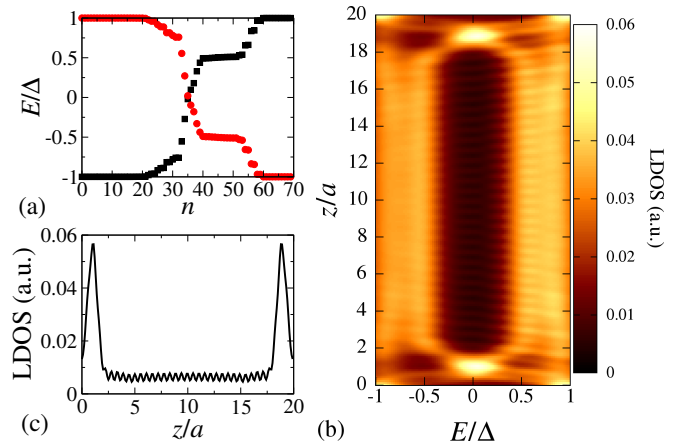


Figure 3. (Color online) Results from the numerical calculation of the YSR states at the wire-like impurity. (a) Distribution of energies of the spin- \downarrow (black squares) and spin- \uparrow (red circles) YSR states. (b) Variation of the energy-resolved local density of states (LDOS) as a function of position z along the wire. (c) Zero-energy LDOS as a function of position z along the wire. We take the same potential for the wire as in Fig. (2). The length of the wire is chosen to be $L = 20a$, and the Fermi wavevector is related to the wire radius by $k_F a = 6$. We restrict the expansion of the T matrix to angular momentum channels with $l \leq 70$.

scale of this reconstruction by modelling the YSR band near the van Hove singularity with the effective Hamiltonian $H = -\hbar^2 \partial_z^2 / 2\tilde{m} + (z - z_0)V_0$, where the linear potential accounts for the movement the van Hove singularity which crosses zero energy at $z = z_0$. The zero-energy solution is an Airy function $\text{Ai}([z - z_0]/l_{\text{eff}})$, with characteristic length scale $l_{\text{eff}} = (\hbar^2 / 2\tilde{m}V_0)^{1/3}$. Estimating the effective mass $\tilde{m} \sim k_F^2 / \Delta$ and the rate of change in the position of the van Hove singularity $V_0 \sim \Delta k_F$, we hence deduce that the peak in the LDOS will be localized over a region comparable to $l_{\text{eff}} \sim k_F^{-1}$. The peak at zero energy is expected to be particularly pronounced, due to the constructive effect of the crossing of the van Hove singularities of the spin- \uparrow and \downarrow branches.

Numerical results: The semiclassical theory above gives an intuitive picture of the YSR physics of the ferromagnetic wire. Here we confirm the appropriateness of this argument by numerical computation of the scattering matrix using a T -matrix approach, and furthermore calculate the variation of the LDOS along the wire.

Our starting point is the relationship between the scattering matrix S and the T matrix [28]

$$S_{l,m,\sigma;l',m',\sigma} = \delta_{l,m;l',m'} - 4\pi i k_F \langle l, m | T_\sigma | l', m' \rangle, \quad (13)$$

where $\langle \mathbf{r} | l, m \rangle = j_l(k_F r) Y_l^m(\hat{\mathbf{r}}) / \sqrt{2\pi}$. The T -matrix for spin- σ scattering is formally given by $T_\sigma = V_\sigma [1 - G_0 V_\sigma]^{-1}$, where $G_0(\mathbf{r}, \mathbf{r}') = -e^{ik_F |\mathbf{r} - \mathbf{r}'|} / 4\pi |\mathbf{r} - \mathbf{r}'|$ is the free Green's function. The T matrix is evaluated numerically by expanding the Green's function and potential in terms of angular momentum eigenstates on a real-space grid inside the wire. Having calculated the scattering

matrix, we then use Eq. (7) to obtain the bound state energy levels, which are plotted in Fig. (3)(a). There is excellent agreement with the bulk semiclassical results in Fig. (2)(a). Focusing on the spin- \uparrow sector, we see that the sharp cluster of states at $\approx -0.5\Delta$ corresponds to the $k_z = 0$ van Hove singularity, while the less pronounced clustering about $\approx 0.8\Delta$ matches the features at $0.5 \lesssim k_z/k_F \lesssim 0.8$. The states with energy just inside the gap are nearly-free and do not significantly contribute to the LDOS in the wire.

To obtain the LDOS we must compute the wave functions within the impurity. Within the T -matrix formalism, the scattering wavefunction $|\psi\rangle$ is related to the bare wavefunction $|\phi\rangle$ by $|\psi\rangle = (1 - G_0V)^{-1}|\phi\rangle$. In particular, we obtain the bound states by choosing $\phi_n(\mathbf{r}) = \sum_{l,m} a_{n;l,m} \langle \mathbf{r}|l,m\rangle$, where a_n is the n th eigenvector of Eq. (7) corresponding to a state with energy E_n . The particle- and hole-components of the bound state wave functions are then given by

$$u_n(\mathbf{r}) = \sum_{lm} \langle \mathbf{r}|(1 - G_0V_\uparrow)^{-1}|l,m\rangle a_{n;l,m}, \quad (14a)$$

$$v_n(\mathbf{r}) = \sum_{lm} \langle \mathbf{r}|(1 - G_0V_\downarrow)^{-1}|l,m\rangle a_{n;l,m}. \quad (14b)$$

Summing over the bound states and integrating over the direction perpendicular to the wire axis, we obtain the LDOS as a function of the position along the wire

$$\rho(z, E) = \int d^2r_\perp \sum_n \{ |u_n(\mathbf{r})|^2 \delta(E - E_n) + |v_n(\mathbf{r})|^2 \delta(E + E_n) \} \Theta(a(z) - |\mathbf{r}_\perp|). \quad (15)$$

In evaluating the LDOS, we include thermal broadening of the δ -functions at a temperature $k_B T = 0.1\Delta$.

We plot the LDOS in Fig. (3)(b). In the bulk of the wire (i.e. $2a < z < 18a$) the LDOS shows very weak z -dependence. The main features are broad peaks centered at $|E| \approx 0.5\Delta$ and 0.8Δ , which correspond to the van Hove singularities of the wire-limit bands. Within the ellipsoidal end caps (i.e. $z < 2a$, $z > 18a$), however, there is substantial modification of the LDOS. In particular, the peaks at $\pm 0.5\Delta$ move towards $\mp\Delta$, and their crossing at zero energy gives a strong peak in the LDOS, as anticipated above. The zero-energy LDOS along the wire is shown in Fig. (3)(c), which reveals that this peak is sharply localized at the ends of the wire.

Our results show strong qualitative resemblance to the experimental data presented in Ref. 18. In particular, we reproduce the subgap peaks in the bulk of the wire and the sharply localized zero-bias peaks at the wire ends. In our model, however, the latter feature does not arise from a bound state (Majorana or otherwise) distinct from the bulk YSR bands, but rather originates from the shifting of the bulk bands at the ends of the wire. We emphasize that the zero-energy peak in the LDOS at the wire end is rather generic, requiring only that the impurity potential be strong enough that the van Hove singularities of the

YSR bands cross zero energy as the radius of the wire vanishes. This zero-energy LDOS feature at the wire ends is not connected to any bound states in the system.

Majorana modes in spin-orbit coupled wires: So far we have restricted our attention to purely ferromagnetic wire-like impurities. Proposals to realize a topologically non-trivial state in such a wire, however, require SOC either within the wire [29] or the superconductor [22, 24]. Here we show how to modify our semiclassical formalism to account for a hypothetical SOC in the ferromagnetic wire. The effect of SOC in the superconducting host on YSR states at a spherical impurity was studied in Ref. 30.

Neglecting the z -dependence of the wire profile, we generalize the scattering matrix Eq. (9) and its time-reversed form Eq. (10) as

$$S_m(k_z) = e^{ib_{0,m}(k_z)} e^{i\mathbf{b}_m(k_z) \cdot \boldsymbol{\sigma}}, \quad (16)$$

$$\tilde{S}_m(k_z) = e^{ib_{0,m}(-k_z)} e^{-i\mathbf{b}_m(-k_z) \cdot \boldsymbol{\sigma}}, \quad (17)$$

where the orientation of $\mathbf{b}_m(k_z)$ now depends on k_z due to the SOC in the impurity. Restricting our attention to a mirror-symmetric geometry, we can choose $b_{0,m}(k) = b_{0,m}(-k)$ and $\mathbf{b}_m(k) = b_m(k) \sin \theta_m(k) \mathbf{x} + b_m(k) \cos \theta_m(k) \mathbf{z}$ where $b_m(k) = b_m(-k)$ and $\theta_m(k) = -\theta_m(-k)$ is the angle of the momentum-dependent magnetic moment with the wire axis. Equation (7) can then be solved to obtain the YSR bands

$$\tilde{E}_{m,\pm}(k_z) = \pm \Delta \sqrt{1 - \cos^2 \theta_m(k_z) \sin^2 b_m(k_z)}. \quad (18)$$

The SOC acts like an effective odd-parity superconducting pairing potential [15], opening gaps in the spectrum of the ferromagnetic wire.

The wire with SOC is in the symmetry class D , which is characterized by a \mathbb{Z}_2 topological number, specifically a Pfaffian. In our semiclassical model this is determined by the spectrum at $k_z = 0$ where $\theta(k_z) = 0$. Since the SOC is irrelevant here, the Pfaffian $W = \text{sgn}\{E_{0,\uparrow}(k_z = 0)\}$, where $E_{m,\sigma}(k_z)$ is the dispersion in the absence of spin-orbit coupling [Eq. (11)]. The topologically non-trivial state corresponds to $W = -1$. From Fig. (2) we see that for the parameters chosen in our numerical study, adding SOC would place the wire in the topological regime, allowing it to support Majorana modes at its ends. These zero-energy Majorana modes would appear in the background of the low-energy LDOS in Fig. (3)(b). At finite temperatures, however, all these subgap features will broaden considerably making experimental interpretation difficult [20].

Conclusions. In this letter we have studied the appearance of YSR states in a wire-like ferromagnetic impurity embedded in a conventional superconductor. Such systems are currently of great interest as a possible platform for realizing Majorana modes [18–21]. Using the normal state scattering matrices, we have examined the YSR states of the wire with both analytical and numerical methods. We find that the YSR bands typically display van Hove singularities, which appear as pronounced peaks in the wire LDOS, and which move towards the gap

edges at the ends of the wire. For sufficiently strong magnetic scattering, the crossing of the two YSR branches near the wire ends gives rise to sharply-localized features in the LDOS at zero energy. Addition of SOC in the wire can stabilize a topological regime, but any Majorana features would appear in the background of an already elevated LDOS near the wire ends. The localized zero-energy peak in the LDOS obtained in our analysis is qualitatively consistent with the recent STM measurements [18] and is independent of the existence of Majorana modes. A conclusive demonstration of Majorana

modes will need to distinguish them from the zero-energy conductance feature presented here.

ACKNOWLEDGMENTS

We thank A. Akhmerov, S. Das Sarma, H.-Y. Hui, A. M. Lobos, R. M. Lutchyn, and D. Rainis for useful discussions. This work is supported by JQI-NSF-PFC and Microsoft Q.

-
- [1] L. Yu, *Acta Phys. Sin.* **21**, 75 (1965).
 [2] H. Shiba, *Prog. Theor. Phys.* **40**, 435 (1968).
 [3] R. I. Rusinov, *Sov. Phys. JETP Lett.* **9**, 85 (1969).
 [4] A. Yazdani, B. A. Jones, C. P. Lutz, M. F. Crommie, and D. M. Eigler, *Science* **275**, 1767 (1997).
 [5] S.-H. Ji, T. Zhang, Y.-S. Fu, X. Chen, X.-C. Ma, J. Li, W.-H. Duan, J.-F. Jia, and Q.-K. Xue, *Phys. Rev. Lett.* **100**, 226801 (2008).
 [6] A. V. Balatsky, I. Vekhter, and J.-X. Zhu, *Rev. Mod. Phys.* **78**, 373 (2006).
 [7] K. J. Franke, G. Schulze, and J. I. Pascual, *Science* **332**, 940 (2011).
 [8] N. Y. Yao, L. I. Glazman, E. A. Demler, M. D. Lukin, and J. D. Sau, *Phys. Rev. Lett.* **113**, 087202 (2014).
 [9] T.-P. Choy, J. M. Edge, A. R. Akhmerov, and C. W. J. Beenakker, *Phys. Rev. B* **84**, 195442 (2011).
 [10] S. Nadj-Perge, I. K. Drozdov, B. A. Bernevig, and A. Yazdani, *Phys. Rev. B* **88**, 020407 (2013).
 [11] J. Klinovaja, P. Stano, A. Yazdani, and D. Loss, *Phys. Rev. Lett.* **111**, 186805 (2013).
 [12] F. Pientka, L. I. Glazman, and F. von Oppen, *Phys. Rev. B* **88**, 155420 (2013).
 [13] S. Nakosai, Y. Tanaka, and N. Nagaosa, *Phys. Rev. B* **88**, 180503 (2013).
 [14] A. Heimes, P. Kotetes, and G. Schön, *Phys. Rev. B* **90**, 060507 (2014).
 [15] P. M. R. Brydon, H.-Y. Hui, and J. D. Sau, *arXiv:1407.6345* (2014).
 [16] Y. Peng, F. Pientka, L. I. Glazman, and F. von Oppen, *arXiv preprint arXiv:1412.0151* (2014).
 [17] C. Nayak, S. H. Simon, A. Stern, M. Freedman, and S. Das Sarma, *Rev. Mod. Phys.* **80**, 1083 (2008).
 [18] S. Nadj-Perge, I. K. Drozdov, J. Li, H. Chen, S. Jeon, J. Seo, A. H. MacDonald, B. A. Bernevig, and A. Yazdani, *Science* **346**, 602 (2014).
 [19] H.-Y. Hui, P. M. R. Brydon, J. D. Sau, S. Tewari, and S. D. Sarma, *arXiv preprint arXiv:1407.7519* (2014).
 [20] E. Dumitrescu, B. Roberts, S. Tewari, J. D. Sau, and S. D. Sarma, *arXiv:1410.5412* (2014).
 [21] J. Li, H. Chen, I. K. Drozdov, A. Yazdani, B. A. Bernevig, and A. H. MacDonald, *Phys. Rev. B* **90**, 235433 (2014).
 [22] P. A. Lee, *arXiv:0907.2681* (2009).
 [23] S. B. Chung, H.-J. Zhang, X.-L. Qi, and S.-C. Zhang, *Phys. Rev. B* **84**, 060510 (2011).
 [24] M. Duckheim and P. W. Brouwer, *Phys. Rev. B* **83**, 054513 (2011).
 [25] S. Takei and V. Galitski, *Phys. Rev. B* **86**, 054521 (2012).
 [26] J. Wang, M. Singh, M. Tian, N. Kumar, B. Liu, C. Shi, J. K. Jain, N. Samarth, T. E. Mallouk, and M. H. W. Chan, *Nat. Phys.* **6**, 389 (2010).
 [27] N. W. Ashcroft and N. D. Mermin, *Solid State Physics* (Harcourt, Orlando, 1976).
 [28] E. Merzbacher, *Quantum Mechanics* (John Wiley & Sons, New York, 1998).
 [29] J. D. Sau, S. Tewari, R. M. Lutchyn, T. Stanescu, and S. Das Sarma, *Phys. Rev. B* **82**, 214509 (2010).
 [30] Y. Kim, J. Zhang, E. Rossi, and R. M. Lutchyn, *arXiv:1410.4558* (2014).